INTEGRATED FERROELECTRICS
2016, VOL. 174, 56–62
http://dx.doi.org/10.1080/10584587.2016.1190598

Taylor & Francis
Taylor & Francis Group

Structural characterization of $(Bi_{1-x}Gd_x)_{14}W_2O_{27}$ ($x = 0.00$ and 0.05) synthesized via mechano-thermal treatment

R. T. Santiago[a], D. S. Vieira[a], R. L. Biagio[a], V. G. Camargo[a], C. F. C. Machado[a], M. Fabián[b], K. L. da Silva[a,b], and V. Šepelák[b]

[a]Department of Physics from Materials, Maringá State University, Maringá, Brazil; [b]Institute of Nanotechnology, Karlsruhe Institute of Technology, Eggenstein-Leopoldshafen, Germany

ABSTRACT

Samples of $(Bi_{1-x}Gd_x)_{14}W_2O_{27}$ ($x = 0$ and 0.05) compounds were prepared via a combination of mechanochemical and thermal treatments upon a $Bi_2O_3/WO_3/Gd_2O_3$ stoichiometric mixture of precursors. Phase evolution, as well as the determination of structural parameters in as-prepared compounds, were performed by XRD analysis. Rietveld refinement revealed that gadolinium ions are incorporated into the tetragonal structure of $Bi_{14}W_2O_{27}$ with preference to occupy octahedrally coordinated Bi^{3+} sites. The Gd doping induced an increase in Bi sites coordination, *i.e.*, the number of oxygens around Bi/Gd ions increased, which can be explained by the absence of $6s^2$ lone pair electrons in gadolinium ions.

ARTICLE HISTORY
Accepted 15 January 2016

KEYWORDS
Bismuth tungstate; X-ray diffraction; Rietveld refinement; lone pair electron $6s^2$

Introduction

Recently, great attention is being devoted to the study of transition metal oxides. Bi_2O_3-WO_3 binary oxides, for instance, have drawn the attention of many scientists because of their complex properties including ionic conductivity, ferroelectricity and piezoelectricity [1, 2].

Among others, BiW_nO_{3n+3} has aroused great interest since its discovery. It posseses an Aurivillius structure, *i.e.* a form of perovskite represented by the generic form $(Bi_2O_2)(A_{n-1}B_nO_{3n+1})$, where A belongs to a large 12-coordinate cation and B to a small 6-coordinate cation. Since perovskite may be structured in layers, the Aurivillius structure is basically built by the alternate layers of perovskite and blocks of a pseudo-perovskite [3].

$Bi_{14}W_2O_{27}$ is characterized by a tetragonal structure ($I4_1/a$) with $a = b = 12.5143(5)$ Å and $c = 11.2248(6)$ Å [4]. This system has three Bi sites assigned to $Bi^{(1)}$, $Bi^{(2)}$ and $Bi^{(3)}$ for 12-fold, 5-fold and 6-fold coordinations, respectively. The doping by gadolinium ions changes the original structure in an irreversible way, leading to a reduction of Bi^{3+} [1]. Focusing on the latter effect, the present

CONTACT K. L. da Silva silvaklebson@dfi.uem.br
Color versions of one or more of the figures in the article can be found online at www.tandfonline.com/ginf.

work aims at evidencing the electrochemical reaction between the gadolinium and the bismuth tungstate ($Bi_{14}W_2O_{27}$) and establishing how gadolinium influences the original structure, how it replaces the bismuth ions and the proportions at which the effect occurs. A doping amount of 5% of gadolinium was used in the initial structure and the $Bi_{14}W_2O_{27}$ and $(Bi_{0.95}Gd_{0.05})_{14}W_2O_{27}$ compounds were analysed.

The main contributions of this work are related to the preparation of the new $(Bi_{0.95}Gd_{0.05})_{14}W_2O_{27}$ phases and to the explanation of how the insertion of Gd ions in the tetragonal ($I4_1/a$) structure can change the Bi site coordinations, *i.e.*, the increase in the coordination number for the two Bi ion sites ($Bi^{(2)}$ and $Bi^{(3)}$).

Experimental

Polycrystalline $(Bi_{1-x}Gd_x)_{14}W_2O_{27}$ ($x = 0.00$ and 0.05) samples were prepared from mixtures of Bi_2O_3 (Alfa Aesar, 99.99%), WO_3 (Alfa Aesar, 99.99%) and Gd_2O_3 (Alfa Aeser, 99.99%). The precursors were mixed in stoichiometric proportions and ground by high-energy ball milling with subsequent thermal treatment. The milling process was conducted for 48 hours at 400 rpm with a ball:powder weight ratio of 30:1 in free atmosphere, using a high-energy planetary ball mill with hardened steel balls and vial. The as-milled powders were annealed at 650 °C ($x = 0.00$) and 800 °C ($x = 0.05$) in free atmosphere for two hours.

In this context, it should be highlighted that the combination of mechanochemical and thermal processes represents a simple, high-yield procedure that reduces the cost and allows completing the synthesis in shorter times [5, 6].

The structural analyses were carried out by powder X-ray diffraction performed with a XRD-6100 Shimadzu X-ray diffractometer operating in a Bragg-Brentano configuration with *Cu-Kα* radiation ($\lambda = 1.54056$ Å). The X-ray diffractograms were performed within the range of 20° to 80° (2θ), using a step size of 0.02° (2θ). The Rietveld structural refinements were performed using the Fullproff Suite [7].

Results and discussions

Rietveld refinements of the X-ray diffraction pattern of $(Bi_{1-x}Gd_x)_{14}W_2O_{27}$ solid solutions prepared by the mechanochemical/thermal synthesis for $x = 0.00$ and 0.05 are shown in Figure 1. The solid curve (black color) represents the fit according to the refinement. The full circles (red color) are the observed X-ray diffraction data and, at the bottom, the difference between observed and calculated intensities is shown (lower continued line, blue color).

In Figure 1(a), the XRD patterns of the as-prepared sample is characterized by sharp peaks corresponding mostly to the tetragonal $Bi_{14}W_2O_{27}$ structure with space group $I4_1/a$. Moreover, tiny peaks on the XRD pattern are attibuted to the $Bi_{12.8}O_{19.2}$ and $Bi_2O_{3.96}$ secondary phases [8–10], with very small phase contributions. The Rietveld analysis revealed for $x = 0.00$ a weight contribution of 99.53% for the predominant $Bi_{14}W_2O_{27}$ phase, while the secondary phases $Bi_{12.8}O_{19.2}$ and $Bi_2O_{3.96}$

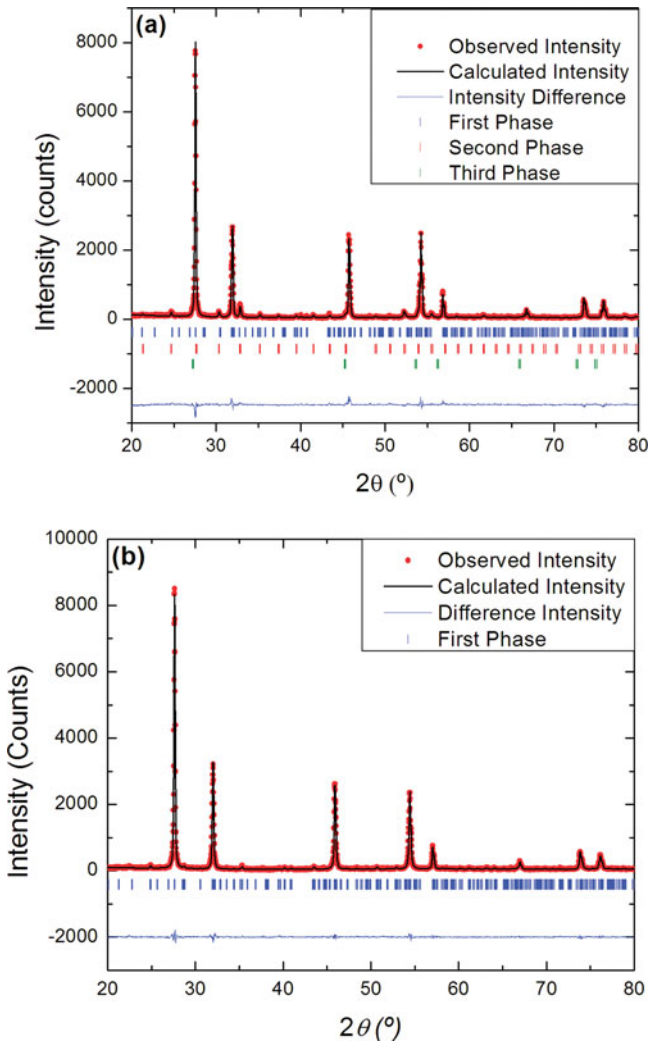

Figure 1. Rietveld refinement of (a) $Bi_{14}W_2O_{27}$ and (b) $(Bi_{0.95}Gd_{0.05})_{14}W_2O_{27}$.

contribute with 0.46% and 0.01%, respectively. The formation of secondary phases is probably due to Bi_2O_3, which evaporates in small amounts when submitted to high temperature. In that case, the initial precursors were not in stoichiometric proportions.

Figure 1(b) shows the XRD structural refinement of $(Bi_{0.95}Gd_{0.05})_{14}W_2O_{27}$. In that case all diffraction peaks correspond to the tetragonal $Bi_{14}W_2O_{27}$ structure with space group $I4_1/a$, thus showing no evidence of secondary phases. Therefore, the combined mechanochemical/thermal process results in a pure $(Bi_{0.95}Gd_{0.05})_{14}W_2O_{27}$ solid solution.

Information on the Rietveld refinement of Figure 1(a) and 1(b), crystallographic data, and *R*-values are listed in Tables 1 and 2.

As it is seen, the introduction of gadolinium in the undoped wolframate structure stabilizes the compound and eliminates the secondary phases. In addition, the

Table 1. Crystal structure parameters for $Bi_{14}W_2O_{27}$.

Empirical Formula		$Bi_{14}W_2O_{27}$		
Crystal System		Tetragonal		
Space Group		$I4_1/a$		
a (Å)		12.5231(5)		
c (Å)		11.2430(5)		
Atomic Positions	x/a	y/b	z/c	O.C.C.
$W^{(1)}$	0.00000	0.00000	0.00000	1.00000
$W^{(2)}$	0.00000	0.00000	0.50000	0.25000
$Bi^{(1)}$	0.00000	0.00000	0.50000	0.75000
$Bi^{(2)}$	0.31040	0.09424	0.00000	4.00000
$Bi^{(3)}$	0.19870	0.39971	0.00000	4.00000
$O^{(1)}$	0.03937	0.04668	0.46550	3.37600
$O^{(2)}$	0.04957	0.37015	0.12500	3.37600
$O^{(3)}$	0.25000	0.25000	0.12500	3.37600
$O^{(4)}$	0.55332	0.14372	0.12500	3.37600
$O^{(5)}$	0.68720	0.05000	0.12500	3.37600
Agreement Parameters (%)	$R_p = 16.3$	$R_{wp} = 18.0$	$R_{Exp} = 12.0$	$\chi^2 = 2.27$

structure of $(Bi_{0.95}Gd_{0.05})_{14}W_2O_{27}$ still possesses a tetragonal structure with space group $I4_1/a$. The lattice parameters become slightly smaller due to the replacement of the Bi^{3+} by Gd^{3+} ions, which possess a smaller ionic radius in the polyhedron unit. Moreover, from the Rietveld analysis, it can be observed that Gd^{3+} has stronger preference to replace Bi^{3+} in the $Bi^{(3)}$ site coordinations (see Table 2).

Figures 2 and 3 illustrate the crystal structure of $Bi_{14}W_2O_{27}$ and $(Bi_{0.95}Gd_{0.05})_{14}W_2O_{27}$, respectively. In Figure 2(a), the light orange polyhedra represent the $Bi^{(2)}$ ions and their five nearest oxygens, while the bright green polyhedra indicate the $Bi^{(3)}$ ions and their six nearest oxygens. Figure 3(a) illustrates the crystal structure of the doped compound $(Bi_{0.95}Gd_{0.05})_{14}W_2O_{27}$. Once more, the light orange and bright green polyhedra have now six and seven nearest oxygens, respectively. After the introduction of Gd ions in the coordination of both sites, the coordination number suddenly increases. The $Bi^{(2)}/Gd^{(1)}$ site position appears to

Table 2. Crystal structure parameters for $(Bi_{0.95}Gd_{0.05})_{14}W_2O_{27}$.

Empirical Formula		$(Bi_{0.95}Gd_{0.05})_{14}W_2O_{27}$		
Ee		Tetragonal		
Space Group		$I4_1/a$		
a (Å)		12.4864(6)		
c (Å)		11.1972(6)		
Atomic Positions	x/a	y/b	z/c	O.C.C.
$W^{(1)}$	0.00000	0.00000	0.00000	1.00000
$W^{(2)}$	0.00000	0.00000	0.50000	0.25000
$Bi^{(1)}$	0.00000	0.00000	0.50000	0.75000
$Bi^{(2)}$	0.2973(6)	0.1074(5)	− 0.0233(8)	1.90037
$Gd^{(1)}$	0.2973(6)	0.1074(5)	0.0233(8)	0.09963
$Bi^{(3)}$	0.1997(7)	0.4041(5)	0.0078(12)	1.66213
$Gd^{(2)}$	0.1997(7)	0.4041(5)	0.0078(12)	0.33737
$O^{(1)}$	0.250(7)	0.0079(3)	0.206(5)	3.37600
$O^{(2)}$	0.0546(20)	0.331(5)	0.06(3)	3.37600
$O^{(3)}$	0.25000	0.25000	0.12500	3.37600
$O^{(4)}$	0.413(5)	0.151(16)	0.12500	3.37600
$O^{(5)}$	0.81765	0.027(8)	0.12500	3.37600
Agreement Parameters (%)	$R_p = 7.09$	$R_{wp} = 10.3$	$R_{Exp} = 8.48$	$\chi^2 = 1.48$

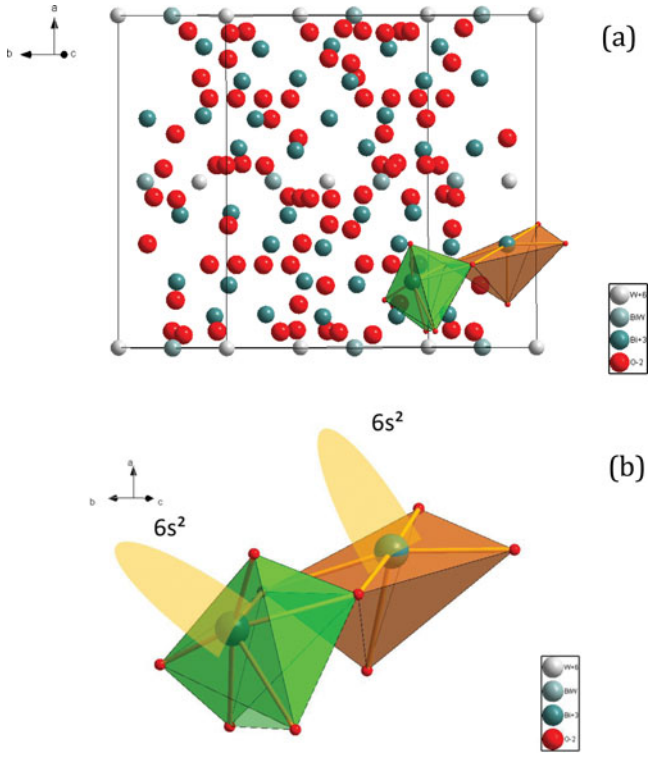

Figure 2. (a) Crystal Structure of $Bi_{14}W_2O_{27}$ (space group $I4_1/a$) with Bi in the 5-fold and 6-fold coordination and (b) representation of the polyhedra with the 6 s^2 lone pair electrons.

have six nearest oxygens, and the $Bi^{(3)}/Gd^{(2)}$ has seven nearest oxygen coordinations. A polyhedron representation for Bi^{3+}/Gd^{3+} situated in both sites for doped and undoped materials is illustrated in Figures 2(b) and 3(b), respectively. In these polyhedra we can observe what the representations with and without the 6 s^2 lone pair electrons for doped and undoped materials look like. For doped material, from the point of view of Rietveld analysis, it is possible to simulate the new polyedron representation with new oxygen coordinations.

The increase of oxygen in the particular polyhedra after Gd doping might be ascribed to the existence of the $6s^2$ lone pair electrons in the Bi^{3+} electronic distribution, which is absent in the Gd^{3+}. In that case, as Gd ions have no 6 s^2 lone pair, it needed to bond with additional electric charge to stabilize the tetragonal struture. For that reason, one oxygen ion approaches the two Gd polyhedra.

After Gd doping in $Bi_{14}W_2O_{27}$, all peaks shift to the higher angles, as expected. In addition, some of these peaks present smaller intensities than the peaks observed in the initial structure, *i.e*, with Gd doping. This is due to the fact that the Gd^{3+} cations possess smaller scattering factors than Bi^{3+} cations. This reflects both the contraction of the crystal lattice and the redistribution of gadolinium ions between the two site positions.

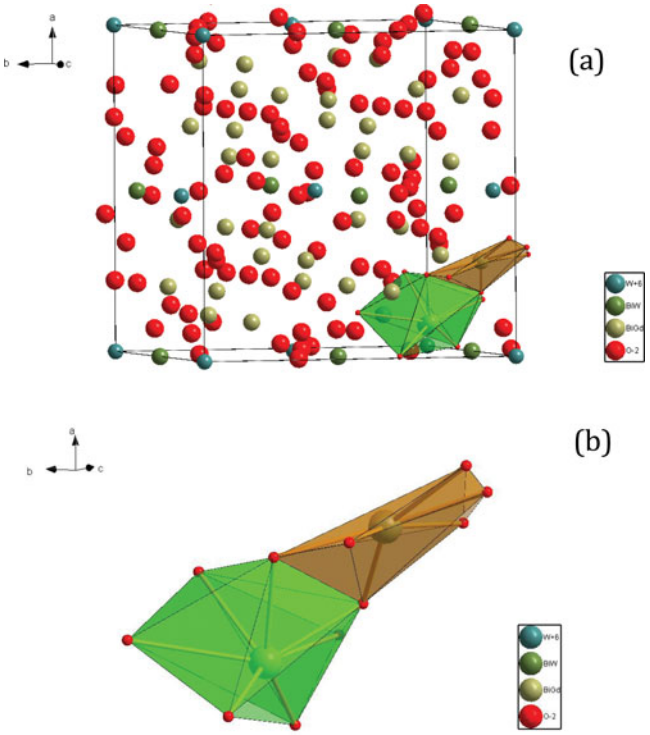

Figure 3. (a) Crystal Structure of $(Bi_{1-x}Gd_x)_{14}W_2O_{27}$ (space group $I4_1/a$) with Bi/Gd in the 6-fold and 7-fold coordinations and (b) representation of the polyhedra without the 6 s^2 lone pair electrons due to Gd substitution.

Conclusions

Polycrystalline $(Bi_{1-x}Gd_x)_{14}W_2O_{27}$ ($x = 0.00$ and 0.05) compounds were prepared from mixtures of Bi_2O_3,WO_3 and Gd_2O_3 by combination of ball milling and thermal processing. The introduction of 5% of gadolinium results in the formation of $(Bi_{0.95}Gd_{0.05})_{14}W_2O_{27}$ without any spurious phases. The new compound crystalizes in the tetragonal structure and belongs to the space group $I4_1/a$. The lattice parameters decrease with Gd doping, since the Gd ion has a smaller ionic radius than the Bi ion. The Rietveld refinement shows that a percentage of Gd ions replace the $Bi^{(2)}$ and the $Bi^{(3)}$ site positions. Nevertheless, Gd ions have a preference to occupy the six-fold coordinated $Bi^{(3)}$ site. The introduction of Gd ions on Bi site position increases the number of coordination, which might be explained by the absence of the 6 s^2 lone pair electrons in Gd^{3+} ions.

References

1. F. E. L. Rodrígues, A. M. De La Cruz, L. T. González, and M. R. González-Quijada Electroquímica de la reacción de litio con el tungstato $Bi_{14}W_2O_{27}$. *Ingenierías.* **14**, 51–52 (2011).
2. G. A. Tompsett, N. M. Sammes, Y. Zhang, and A. Watanabe Characterisation of WO_3,V_2O_5, and P_2O_5-doped bismuth oxides by x-ray diffraction and Raman spectroscopy. *Solid State Ionics.* **113–115**, 631–638 (1998).

3. K. R. Kendall, C. Narvas, J. K. Thomas, and H. C. ZurLoye Recent Developments in Oxide Ion Conductors: Aurivillius Phases. *Chem. Mater.* **8**, 642–649 (1996).
4. A. Watanabe, N. Ishizawa, and M. Kato A outline structure of $7Bi_2O_3$-$2WO_3$ and its solid solutions. *J. Solid State Chem.* **60**, 252–257 (1985).
5. K. L. Da Silva, D. Menzel, A. Feldhoff, C. Kübel, M. Bruns, A. Paesano Jr, A. Düvel, M. Wilkening, M. Ghafari, H. Hahn, F. J. Litterst, P. Heitjans, K. D. Becker, and V. Šepelák Mechanosynthesized $BiFeO_3$ nanoparticles with higly reactive surface and enhanced magnetization. *J. Phys. Chem. C.* **115**, 7209–7217 (2011).
6. Da Silva K. L., V. Šepelák, A. Düvel, Paesano AJr, H. Hahn, F. J. Litterst, P. Heitjans, and K. D. Becker Mechanochemical-thermal preparation and structural studies of mullite-type $Bi_2(Ga_xAl_{1-x})_4O_9$ solid solutions. *J. Solid State Chem.* **184**, 1346–1352 (2011).
7. J. Rodriguez-Carvajal Fullprof Program, version 2.4.2, ILL Grenoble, Grenoble, France, 1993.
8. M. Nespolo, A. Watanabe, and Y. Suetsugu Re-investigation of the structure of 7(Bi2O3)–2(WO3) by single-crystal X-ray diffraction. *Cryst Res and Technol.* **37**, 414–422 (2002).
9. H. A. Harwig On the structure of bismuthsesquioxide: the α, β, γ and δ-phase. *Zeitschriftfüer Anorganische und Allgemeine Chemie.* **444**, 151–166 (1978).
10. S. F. Radaev, V. I. Simonov, and Kargin YuF Structural features of the γ-phase Bi_2O_3 and its place in the sillenite family. *Acta Cryst.* **B48**, 604–609 (1992).